Available online at www.jrors.ir

Journal Of Radar and Optical Remote Sensing

JRORS 1 (2019) 46–57

Detecting and Calculating the Soil Moisture Using Microwave Imagery (Case Study: Miyankale, Mazandaran)

Abolfazl Rahimabadi[a *], Ali Akbar Jamali[b]

[a]*Department of GIS & RS, Yazd Branch, Islamic Azad University, Yazd, Iran*
[b]*Associate Professor, Department of GIS-RS and Natural Engineering, Maybod Branch, Islamic Azad University, Yazd, Iran*

Received 2 March 2019; revised 26 May 2019; accepted 30 May 2019

Abstract

Almost one third of the earth is covered by soil, which has several essential parameters. The soil moisture content is one of the essential parameters. The current research calculates the soil moisture content. There are known methods to calculate soil moisture; however, a new method has been chosen for this research. Microwave imagery is a novel appropriate way to detect and calculate the amount of moisture in soil. The SENTINEL-1 with SAR sensor has been a good satellite for research purpose. The microwaves sent by the satellite to the earth receives the backscatters which has been directly related to the amount of moisture. Thus four images were obtained at different time intervals of the year; 21st November 2015, 1st May 2016, 5th June 2016 and 29th September 2016. The study area of Miyankale is covered by four images. Furthermore, to calculate the moisture in Miyankale which was done by another method the results were finally compared with the percentage measured by satellite imagery. The accuracy of satellite data is confirmed by measuring the soil moisture by two different methods. The coefficient of determination R^2 has been chosen to compare the data and check the microwave imagery. The R^2coefficient is able to compare two independent data. The R^2 coefficient is 0.82, 0.82, 0.78 and 0.81 for different time periods. The R^2 ranges from 0 to 1, as the R^2 values are closer to 1 the moisture obtained from SAR images is confirmed

Keywords: Backscatter Coefficient, Soil Moisture, SAR, Sentinel-1

* Corresponding author. Tel:.+98-9359405245.
E-mail address: rahimabadi_abolfazl@yahoo.com.

1. Introduction

One of the soil parameters that would affect other parameters is moisture thus the focus of this research is calculating the amount of moisture of the soil. Although soil moisture has been measured through other researches, this research proposes and examines a novel method. The application of satellite data to measure the amount of moisture in the soil is a new method in Iran. The satellite sends the microwaves to the earth and receives the backscatters which are directly related to the amount of moisture. Few radar practical examinations are there which dedicates the soil parameters such as moisture (Altese et al., 1996). Among various satellite data, radar data is an appropriate data to extract the moisture percent in the soil (Behyar et al., 2014). In other words, radar spectrum is more capable than other electromagnetic spectrum to detect moisture in the soil. Therefore, radar satellite has been chosen to detect the soil moisture (Bao et al., 2018). The Sentinel-1 with SAR sensor, which produces and sends radar waves to the earth and receives the backscatter in return from earth features (Thain et al., 2011). This research choses a new method of radar imagery by downloading several images of Sentinel-1, to calculate the soil moisture. Determination of soil moisture is important for agricultural products (Potin et al., 2011).

The method employed to extract soil moisture will be explained. The images were processed to map soil moisture parameters of the case study and to determine the amount of moisture in each image.

In order to retrieve the soil surface parameters, an algorithm has been investigated and implemented. Soil parameters such as moisture and roughness are used in various fields (Lievens et al., 2017). SAR (Synthetic aperture radar) capability to measure the soil parameters is known for more than 30 years however, scientists are still searching for appropriate sensors and applicable algorithms to restore the soil parameters (Mirmazlumi., 2014). For instance, European Space Agency (ESA) scientists have used radar wavelength with the SMOS (Soil Moisture and Ocean Salinity), in order to measure two variables: soil moisture and salinity of the oceans (Mecklenburg; 2015). Radar images have two sections included power and phase (backscatter), which are used to determine the moisture content of the soil. Literally, the hypothesis of the research is the relation of backscatter and moisture where humidity is expected to be directly related to backscatter. This research has modeled the changes in radar images. Radar wavelengths are able to detect the difference content of the moisture in soil. The main purpose was to employ a new method with a high resolution data, while it benefited the research by decreasing time and cost. Finally, the results obtained with these wavelengths will be analyzed and mapped in the case study of Miyankale.

1.1. Soil Surface Parameters

Generally, soil surface parameters can be subdivided into three categories:

1. Surface roughness parameters: These parameters include the distribution of ground targets, surface profile height, autocorrelation function and surface roughness criteria.
2. Soil properties: Surface roughness, water capacity, depth of penetration and macro-level structure are included in this category.
3. Vegetation characteristics: The vegetation structure and geometry of the plant, along with the water capacity of the plant are the most important parameters of this category (Mirmaslomi, 2014).

1.2 Literature Review

Ebrahim Babayan et al. (2013) used ASAR images to estimate soil moisture content and also TDR humidifier to validate the data. It was concluded that the GM mode of ASAR images is more appropriate to be used in semi-arid and undercoats conditions to estimate soil moisture content. Dr. Entekhabi's methodology was developed in 1994. Dual soil moisture model and heat loss model are employed to measure moisture and surface temperature. These measurements were processed and used to estimate the moisture and then were generalized to the depths of surface. Foson Balik et al. (2008) used the backscatter waves of ASAR, PALSAR and RADARSAT-1 radar sensors, to measure soil moisture 86%, 76% and 81%, respectively. Balik compared different polarizations of three sensors and concluded that in spite of better spatial resolution 30*30 meter of ASAR image, the results are almost the same in the study area Izmir of Turkey. Also, Saloni et al. (2008) compared the accuracy of ASAR images (band C, HH and VV polarization), RADARSAT-1 and PALSAR (L band, HH polarization) to estimate soil moisture content in

agricultural land in western Turkey. According to their results, the relationship between soil moisture content and backscatter coefficient of soil was R^2 = 0.77, 0.81 and 0.86, respectively. In another study, Brocka et al. (2011) used the passive microwave data of the AMSR-E sensor of Aqua satellite and ASCAT sensor of MetOP Satellite to measure moisture content of the soil surface, with correlation coefficients of (R) 0.71 and 62.2, respectively. Baghdadi et al. (2012) estimated the soil moisture content in vegetation-free conditions with a precision of 3% using the TERRASAR-X test data. Lyons and Verhoest (2012) detected the correlation between RADARSAT-2 data in HH and VV polarizations. The IEM^* model estimated the soil moisture content, with the RMSE equal to 0.04 (cubic centimeter per cubic centimeter). Kulas et al. (2016), found improvements in detecting soil moisture in the ranges of 5 to 19 percent. In an investigation which they worked on microwave satellite data for the assessment of soil moisture, it was found that if active satellite (ASCAT) and passive (AMSR) data were used complementarily, a significant improvement would be obtained. Lyons et al. (2017) did the same study by two observations. Both active radar (ASCAT) and passive (SMOS) considered to observe backscatter coefficient and lighting temperature. Lyons found out that combining these parameters would estimate the soil moisture in depth of 0-10 cm with a great accuracy of 0.548.

2. Materials and Methods

The research is based on two types of data; field data and satellite data. The field data examined soil in the case study in order to measure the amount of soil moisture. These field measurements were necessary to be done to compare with the moisture obtained by radar images. In further section would be cleared the relationship between field data and satellite data First of all, the case study has been introduced.

2.1 Study Area

Behshahr city is located in the mountainous foothills of Alborz Mountains with two mountainous and plain areas. It extends from 36 degrees, 45 minutes to 36 degrees and 88 minutes longitude, and 53 degrees and 21 minutes to 54 degrees 13 minutes latitudes. Miyankale Peninsula is located in this city as a plain district next to the Caspian Sea. The Miyankale is a narrow Peninsula where reached to the Caspian Sea from the north, and reached to the narrow, shallow Gorgan Gulf from the south. It restricted by Raghmarz wetland from the west and narrow strait of less than one kilometer in the neighboring port of Turkmen from the east.

The area of Miyankale is a unique area of about 68 thousand hectares. The average altitude of this area is 30 meters below the sea level, and its annual rainfall is 717 mm. Miyankale is located in a warm, humid climate. The terrestrial ecosystem consists of sandy hills of the Pomegranate trees, berry bushes, Sazil (Local vegetation) bushes and grassland region. These various vegetation areas are not uniform and are dense in some hectares but thin in others.

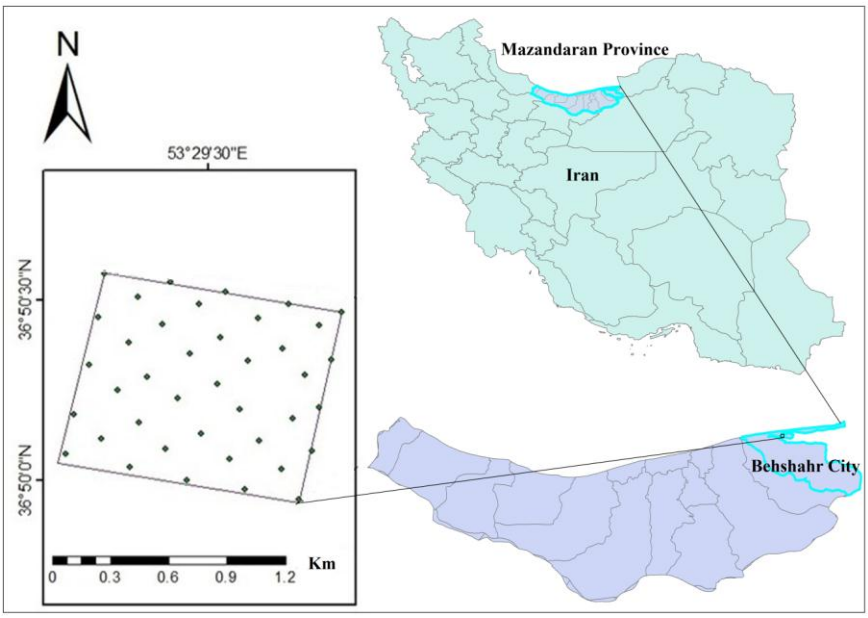

Figure 1. Case study of Behshahr

2.2. Field Data

Besides processing satellite data, the field data were collected in 1 km^2 area, considered to be checked in soil moisture. The observed moisture content was calculated in depth (1-10) centimeters. Forty samples were obtained in different location. The samples were kept in specific metal dish in order to transfer to the soil laboratory. The soil laboratory measured the percentage of moisture content. The location of each sample point was recorded by the GPS device Figure 2. Another point to be noticed is the different types of sampling. The soil differed from sand to gravel and vegetation types in sampling positions varied from thin to dense grass to a height of 10 centimeters. It should be considered that, during software processing, the effect of vegetation was removed.

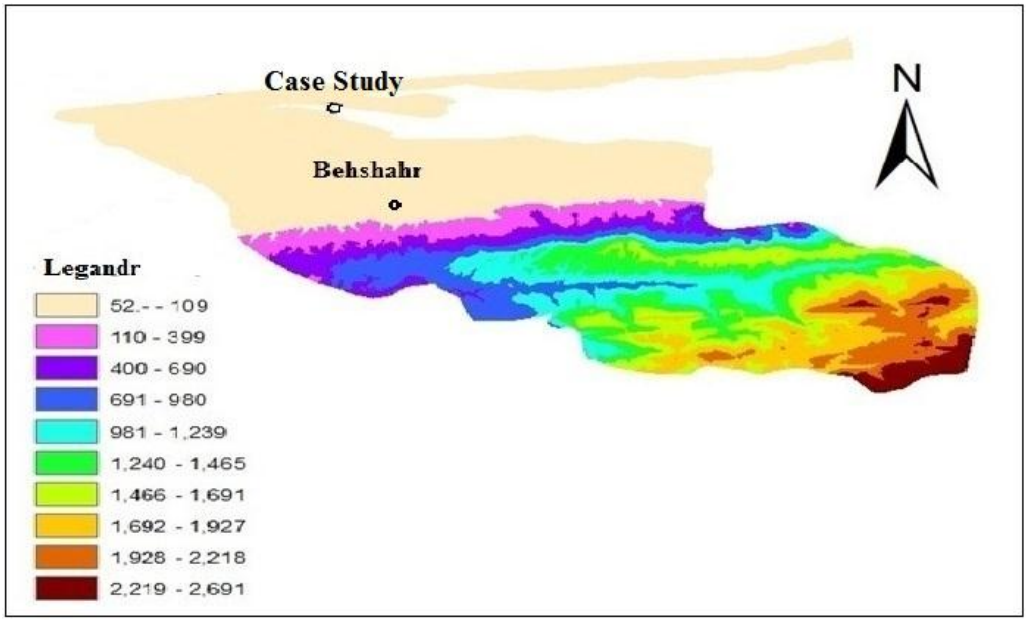

Figure 2.DEM of Behshahr; (Authors)

2.3. Satellite Data

Two satellites were considered to employ their images; LANDSAT-8 and SENTINEL-1. As long as SENTINEL-1received all the radar backscatters from the ground, it was necessary to delete the vegetation backscatter. The impact of vegetation had to be eradicated then the radar images were processed to measure the soil moisture. The NDVI (Normalized Difference Vegetation Index) is a vegetation index which obtained by LANDSAT-8. Three Landsat-8 images were downloaded in approximately the same date of the radar images. LANDSAT-8 images were preprocessed then processed to calculate the vegetation density in the case study of Miyankale Peninsula. The NDVI index was calculated in order to measure, the LAI (Leaf Area Index) equation (1):

$$LAI = 0.57 * \exp(2.33 * NDVI)) \quad (1)$$

In Figure 3 the methodological flowchart of this research is indicated

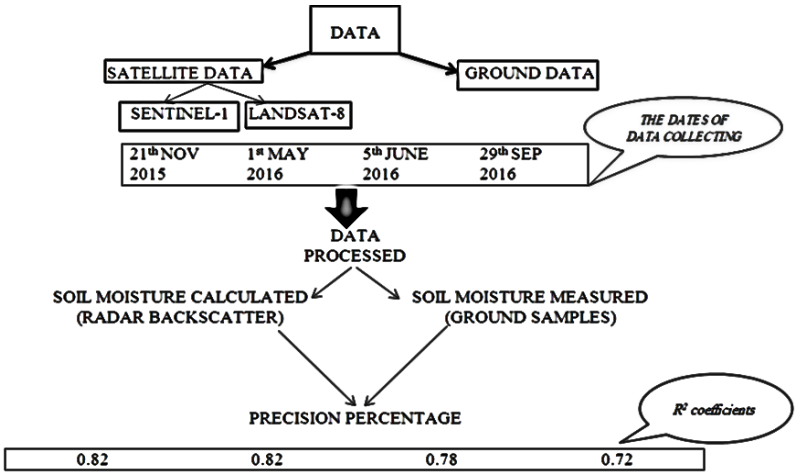

Figure 3. Flowchart of the research (author)

2.4. Methodology

The European Space Agency is an open source to get the Sentinel-1 images. These are high resolution images with a large frame size of 40,000 pixels * 40,000 pixels. First of all orbital correction is exerted to the image. There are two types of correction files, POEORB, RESORB. The RESORB file is easier to access rather than other file. It could be downloaded in less than a day; however, the POEORB orbit took longer period but it was more accurate. Thus the POEORB file was used in this research. The next step was to remove the thermal noise and then the image was calibrated by Sigma0 band. As long as the pixel size is half of the SAR image resolution, the image's speckle was removed by making multilook of the image.

Each pixel is the result of a total of backscatter to the satellite, and each backscatter has a different phase. Therefore, the interference of these waves causes the formation of dark or bright spots in the final image. This created noise, such as salt and pepper, is sprayed on the images; it is an unavoidable error in coherent systems Figure 4.

For each pixel, γ (x, r) is equal to the sum of the backscatter (2):

$$|u(x_0, r_0)| = |\gamma(x_0, r_0) * u_0(x, r)| = |\Sigma\, \gamma_i(x_0, r_0) * u_0(x, r)| \quad (2)$$

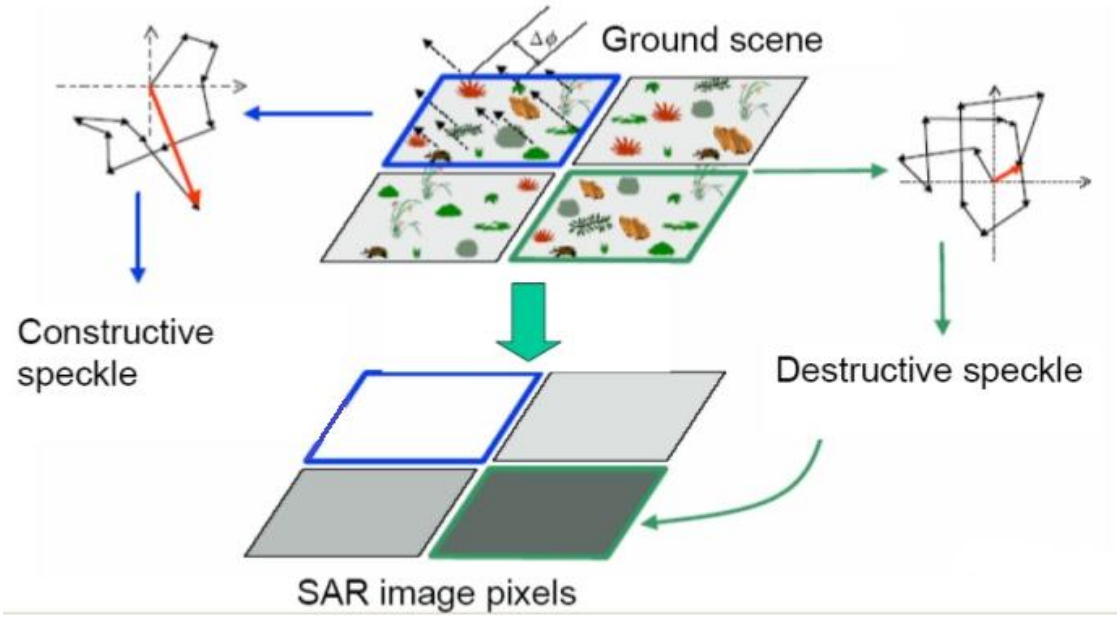

Figure 4. Backscatter of each pixel (Mincla, 2016)

The effects of speckles on the image degraded the quality hence making it more difficult for the interpretation. According to the Figure 5, as the backscatter increased, the speckle would increase too.

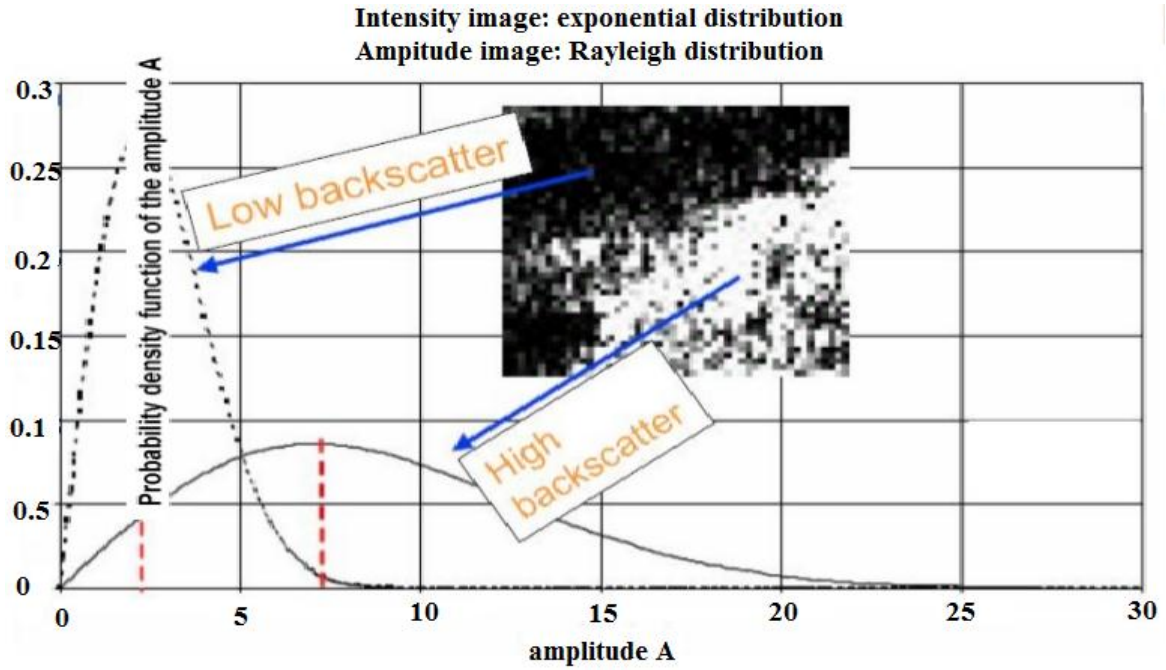

Figure 5. Relationship between word and image and postback (Mincla, 2016)

In this paper, the Moody's filter was used (Babayan, 2013) to remove speckles. As the multilook increased, the probability distribution function narrowed. The narrow function corresponds to the speckle reduction in the image (Mincla, 2016). The speckles of the images were removed using different date of imagery of the same place. In other word, various images of the case study at different time were the solution for detecting speckles. In the next procedure geometric correction, georeference and normalization of the slope of the area were exerted. The slope is corrected by the Band Math operator

shown in quotation (3). Now the sigma zero (Sigma Nought) (σ °) of the region is calculated by multiplying backscatter of the reference ellipse to the sinusoidal fraction in Figure 6. The θ_{DEM} is the angle of the radar wave with the digital elevation model and θ_{ELL} is the angle of the wave with the reference ellipse.

$$\text{Area}: \sigma^{\circ}\text{Norm} = \sigma^{\circ}\text{Ellipsoid} * \frac{\text{Sin}\theta\text{DEM}}{\text{Sin}\theta\text{Ell.}} \quad (3)$$

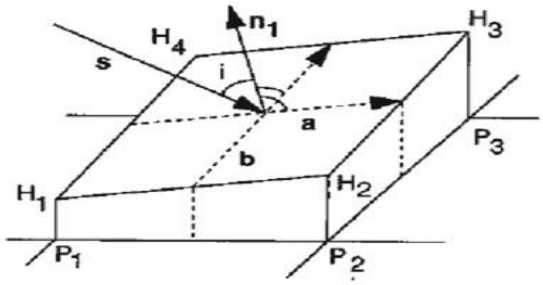

Figure 6. Reflection related with the gradient of its reflection surface (Mincla, 2016)

The radar image is composed of phase or power that should be converted to a user-friendly image. How to display the Sentinel image depends on the received geometry. After processing the image data in Figure 7, it was time to estimate the moisture content and the backscatter relationship with the moisture content of the studied area and vegetation density.

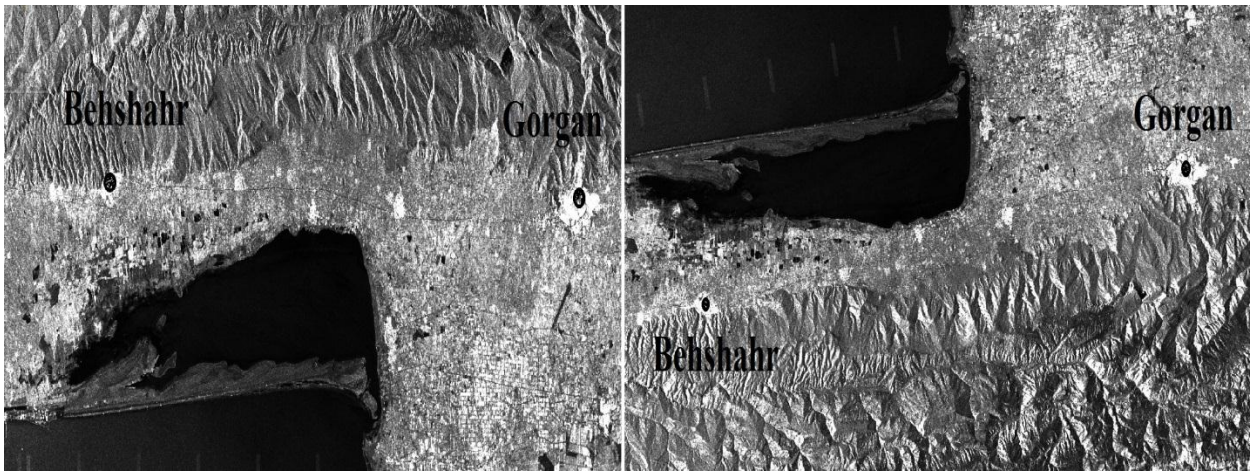

Figure 7. Right image is the final processing (Authors)

The backscatter of the earth surface was obtained using equation (4);Where σ_s° soil backscatter and σ_{dv}° plants backscatter, and also σ_{int}° is the backscatter of the plant and soil. The plant backscatter is derived from equations (5) and (6) where τ^2 is the portion of light which transferred of the vegetation surface and LAI is the leaf area index. The angle θ is declination of the sensor (Moren, 2005).

$$\sigma^{\circ} = \tau\dot{\sigma_s} + \dot{\sigma_{dv}} + \dot{\sigma_{int}} \quad (4)$$

$$\tau^2 = \exp(-2\text{LAI}\sec\theta) \quad (5)$$

$$\dot{\sigma_{dv}} = \text{LAI}\cos\theta(1-\tau^2) \quad (6)$$

3. Results and Discussion

The coefficient of determination, denoted R^2 "R squared", is used to compare independent variable(s). The research had two types of data which were also independent; first group were field measurements and

the second one were images calculation. It should be considered that these two types of data were prepared independently in order to be compared. The calculation of R^2 coefficient is an appropriate method to compare these data. The research chose this method to examine the correctness of moisture percent extracted form SAR imagery. Since the field moisture was measured correctly, the R^2 coefficient determined the correctness of moisture measurements on SAR images. In other words, R^2 is capable of determination of SAR imagery whether it detected the soil moisture in a correct way or not. The coefficient of determination ranges from 0 to 1. As the R^2 value became closer to 1, the moisture obtained from SAR images was confirmed.

3.1. Comparison of Surface Reflection Coefficients and Observation of Humidity

The coefficient (R^2) is 0.82, 0.82, 0.78, 0.72, and 0.81 for different time periods were obtained as shown in Table 1. The difference between these two variables can be due to the backscatter received by the sensor, which included the polarization and the soil's types (Altis, 1996).

The coefficient (R^2) obtained from the diagrams indicated that the coefficient of determination differed from 0.72 to 0.82 due to the moisture content and backscatter in different time series. The least amount of R^2 is for VH polarization. Also, for the coefficient of determination, different results were obtained, which will be described below.

Table 1. Results of RMSE and R^2 coefficient and moisture variables observed in different time series (Authors).

R^2	RMSE	Polarization	Date
0.82	0.35	VV	11/21/2015
0.82	1.06	VV	5/1/2016
0.78	1.49	VV	6/5/2016
0.72	1.75	VH	6/5/2016
0.81	0.68	VV	9/29/2016

3.2. Comparison of Backscatter Coefficient with Vegetation (NDVI)

The relationship between vegetation and wavelength is important in detecting soil moisture, as the wavelength must pass through vegetation as the main obstacle and reach the soil. According to Babaeiyan et al, if the plant biomass is less than 0.5 kg / m^2, the vegetation effect can be ignored on the total backscatter coefficient (Das, 2008). In hot seasons, when the dehydration is high, vegetation is noticeably reduced and less correlated with backscatter. Thus it was proved that C band was affected by vegetation. In the studied area, the effect of vegetation was eliminated due to a variety of vegetation and its effects on backscatter.

3.3. Distribution of Backscatter in Time-Spatial Dimension

The normalized total backscatter was shown in 15 meters pixels during the study period. As seen, the total backscatter was affected by vegetation area. It should be noticed that the backscatter is obtained from the northern, northeastern and western parts of the region as it is shown in Figure 8, where there were more vegetation and thus more soil moisture (Mesri, 2013).

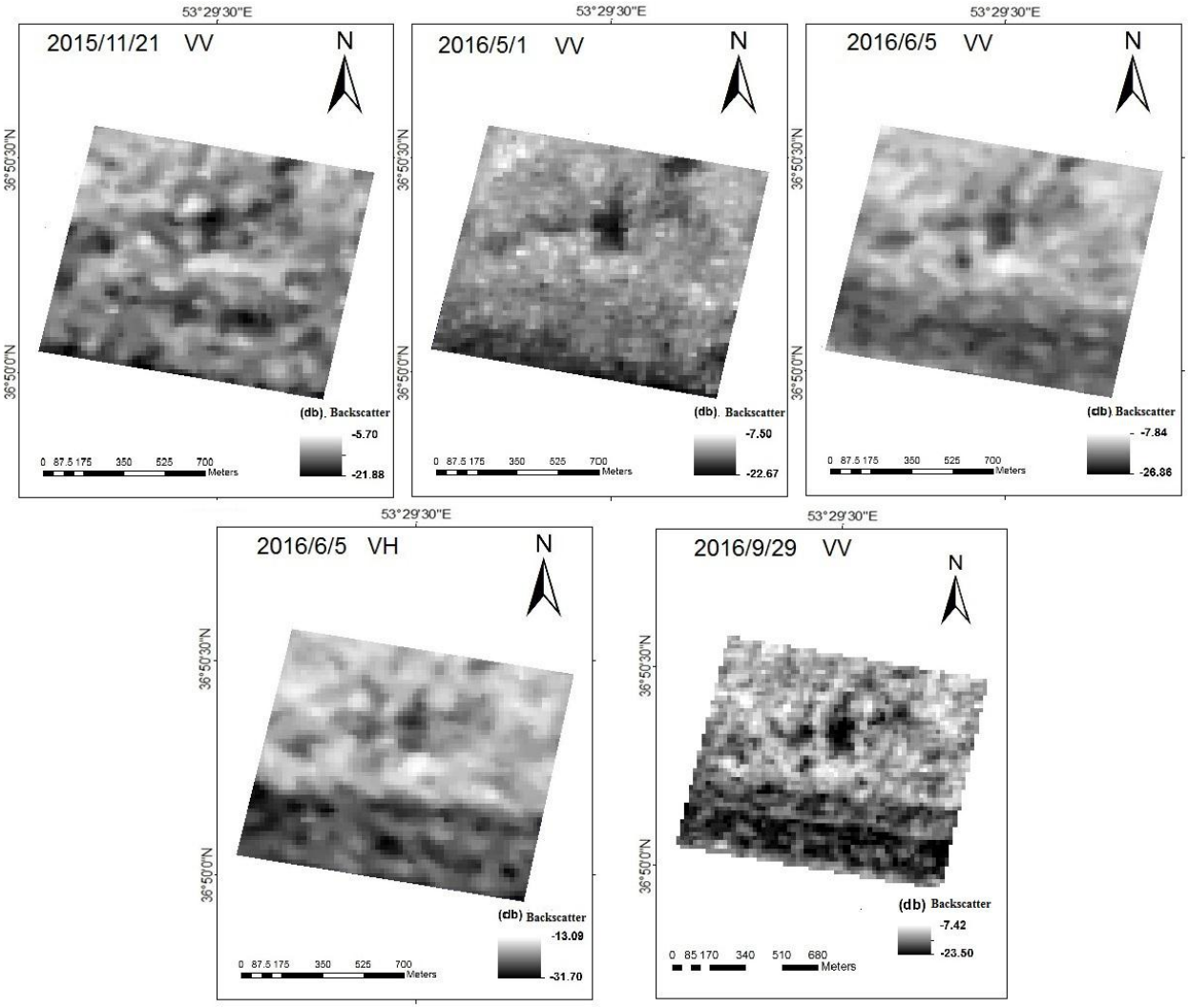

Figure 8. Time-spatial distribution of the total backscatter (1 * 1 km) (Authors)

3.4. Precision Testing

Based on the results, the R^2 value was between 0.72 and 0.82, as well as RMSE between 1.75 and 0.35. The RMSE value was approximately dependent on the month or season of the year. In other words, during low rainfall season, RMSE is somewhat diminished, as the effect of vegetation on backscatter. While Babaian et al. calculated 0.68 for R^2 based on surface soil moisture with ASAR images and HH polarization, the current research results in the VH and VV polarization, were above 0.70%. In addition, Salon et al. calculated moisture content using C-band with HH and VV polarization then reached to R^2 coefficients equal to 0.77, 0.81, and 0.88, which was approximately the same as this research.

In general, region vegetation diversity was very crucial and determined the accuracy of R^2 coefficient. In the study of Nazari Aghdam, with satellite optic data, there was a high correlation between soil moisture content and NDVI. Therefore in this study, there were no needs for images in visible wavelengths. In Khanmohammadi's research, vegetation indices such as NDVI, NDMI and LST employed using MODIS satellite data to extract soil moisture content. Although measuring soil moisture in Khanmohammadi's research definitely affected by vegetation areas; its precision was not good enough compared to this research. According to Figure 9, the moisture content of the whole Mmiyankale Peninsula was mapped based on each image on SAR sensor.

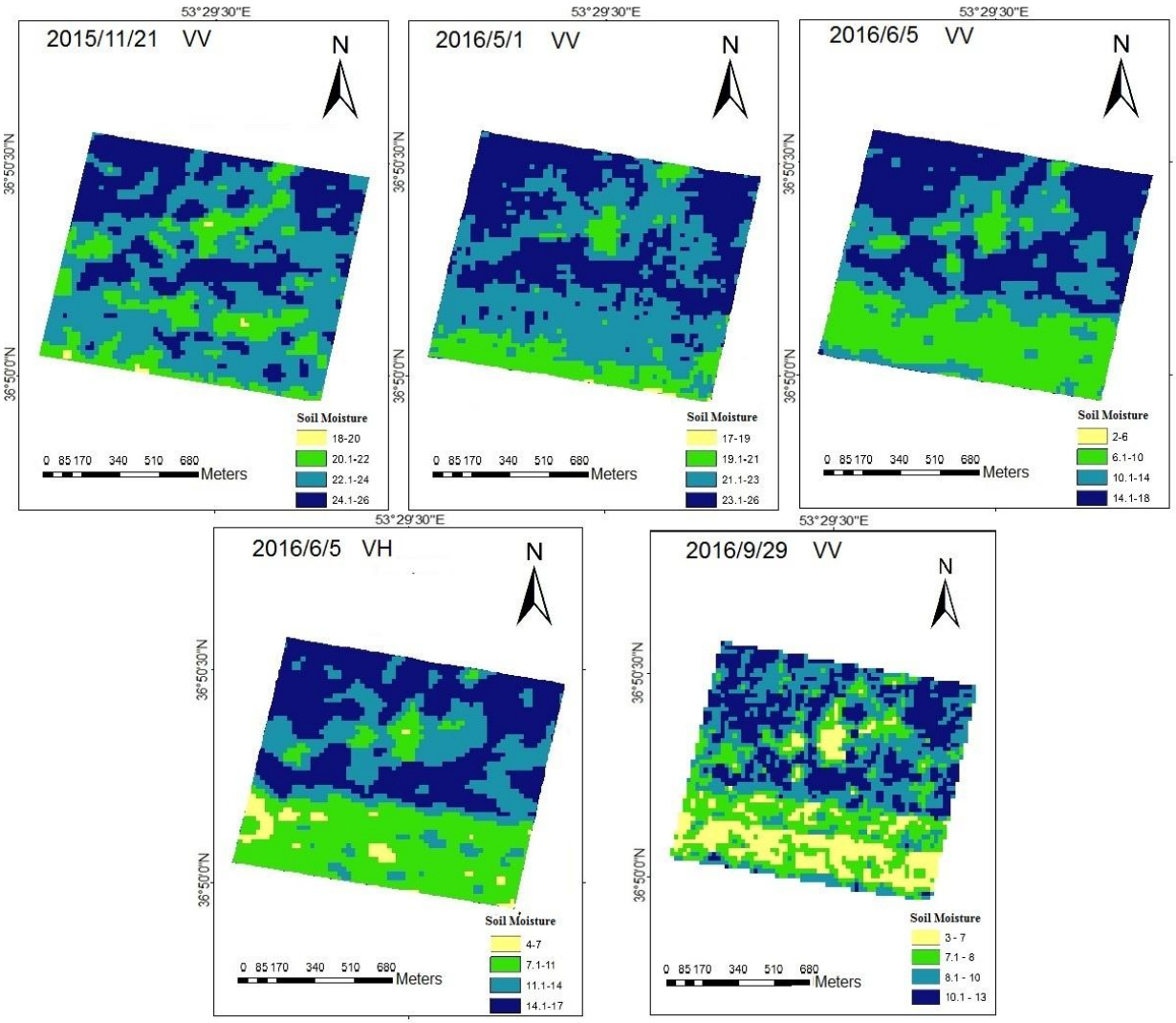

Figure 9. Time-Spatial distribution of soil moisture content 1 * 1 km (Authors)

4. Conclusion

There were a few radar practical examinations which dedicated the soil parameters such as moisture. The radar data is an appropriate data to extract the moisture percent in the soil. In this research, a simple experimental model proposed which was based on the backscatter data in GM mode of the Sentinel satellite. Balik et al. (2008) used the backscatter waves of ASAR, PALSAR and RADARSAT-1 radar sensors, to measure soil moisture 86%, 76% and 81%, respectively. Also, Saloni et al. (2008) compared the accuracy of ASAR images, RADARSAT-1 and PALSAR then figured out the relationship between soil moisture content and backscatter coefficient of soil was R^2 = 0.77, 0.81 and 0.86, respectively. Baghdadi et al. (2012) estimated the soil moisture content in vegetation-free conditions with a precision of 3% using the TERRASAR-X test data. Babayan et al. (2013) used ASAR images to estimate soil moisture content and also TDR humidifier to validate the data. It is concluded that the GM mode of ASAR images is more appropriate to be used in semi-arid and undercoats conditions to estimate soil moisture content. Behyar and Mirmazlumi have done in two independent researches in 2014. Also, Bao has done the same in 2018 by radar satellite to detect the soil moisture.

The current research chose the radar method based on SAR sensor capability to measure soil

parameters. The time-spatial model was proposed to retrieve, monitor, and mapping soil moisture of the earth surface. The regression model estimated the soil moisture content in the study area through the R^2 coefficient and RMSE calculations. The results of the evaluation and validation of the model showed that there is slight difference between the soil moisture content and the measured values. Due to the lack of coherent data of soil moisture in Iran country, especially in crucial agricultural sites, employing the SAR data from the GM model would be an effective novel method. In this regard, it is recommended to use long-wavelength bands for vegetation areas. The coefficient (R^2) is 0.82, 0.82, 0.78, 0.72, and 0.81 for different time periods were obtained as shown in Table 1. The difference between these two variables can be due to the backscatter received by the sensor.

References

Altese, E., Bolognani, O., Mancini, M., & Troch, P.A. (1996). Retrieving soil moisture over bare soil from ERS1 Synthetic Aperture Radar data: sensitivity analysis based on theoretical surface scattering model and field data. *Water Resources Research Journal*, *32*(3), 653-661.

Babayan, A., Homaei, M., & Nowruz, A.S. (2013). Estimation of surface soil moisture using ENVISAT / ASAR radar images. *Water Research in Agriculture Journal, (27)*4, 622-611.

Baghdadi, N., Aubert, M., & Zribi, M. (2012). Use of TerraSAR-X data to retrieve soil moisture over bare soil agricultural fields. *IEEE Geoscience and Remote Sensing Letters*, *9*(3), 512-516.

Bao, J., Hou, Z., Ray, J., Huang, M., Swiler, L., & Ren, H. (2018). Soil moisture estimation using tomographic ground penetrating radar in a MCMC–Bayesian framework. *Stochastic environmental research and risk assessment, 32*(8), 2213-2231.

Behyar, M. B. (2014). Evaluation of Soil Moisture in Isfahan Province by AMSR-E. *Geographical Research (1017-4125), 29*(1).

Brocca, L. S., Hasenauer, T., Lacava, F., Melone, T., Moramarco, W., Wagner, Dorigo, w.(2011).

Assimilation of the ASCAT soil moisture product for flood prediction and forecasting. *EUMETSAT/ESA scatterometer science conference.*

Das, N. N., Mohanty, B. P., & Njoku, E. G. (2008). A Markov chain Monte Carlo algorithm for upscaled SVAT modeling to evaluate sattelite-based soil moisture measurements. *Water Resources Research, 44*(5).

Entekhabi, D., Nakamura, H., & Njoku, E. G. (1994). Solving the inverse problem for soil moisture and temperature profiles by the sequential assimilation of multifrequency remotely sensed observations. *IEEE Transactions on Geoscience and Remote Sensing, 32*(2), 438-448.

Khanmohammadi, F., Homaei, M., & Nowruz, A. S. A. (2014). Estimation of soil moisture using vegetation indices and soil temperature and normalized moisture index using MODIS Images. *Journal of Soil and Water Resources Conservation*, *2*(4), 1-9.

Kolassa, J., Gentine, P., Prigent, C., & Aires, F. (2016). Soil moisture retrieval from AMSR-E and ASCAT microwave observation synergy. Part 1: Satellite data analysis. *Remote Sensing of Environment, 173*, 1–14.

Lievens, H., & Verhoest, N. E. C. (2012). Spatial and temporal soil moisture estimation from RADARSAT-2 imagery over Flevoland, The Netherlands. *Journal of Hydrology*, *456*, 44-56.

Lievens, H., Martens, B., Verhoest, N.E.C. Hahn, S. Reichle, R.H., & Miralles, D.G. (2017). Assimilation of global radar backscatter and radiometer brightness temperature observations to improve soil moisture and land evaporation estimates. *Remote Sensing of Environment 189,* 194–210.

Mecklenburg, S., Drusch, M., Kaleschke, L., Rodriguez-Fernandez, N., Reul, N., Kerr, Y., Font, J., Martin-Neira, M., Oliva, R., Daganzo-Eusebio, E., Grant, J.P., Sabia, R., Macelloni, G., Rautiainen, K., Fauste. J, de Rosnay. P, Munoz-Sabater. J, Verhoest. N, Lievens, H., Delwart, S., Crapolicchio, R., de la Fuente, A., & Kornberg, M. (2015). ESA's Soil Moisture and Ocean Salinity mission: From science to operational applications. *Remote Sensing of Environment, 180,* 3-18.

Minchella, A. (2016). SNAP Sentinel-1 in a Nutshell, – "ESA SNAP-Sentinel-1 Training Course" *Satellite Applications Catapult - Electron Building, Harwell: Oxford*.

Mesri, A., Kamkarrowhani, A., & Arab Amiri, A. (2013). Determination of Soil Moisture Content Using GPR Method and Comparison of Results with Laboratory Results, Case Study: Shahroud University Agricultural University Campus. *8th Conference of Engineering and Environmental Geology of Iran, Ferdowsi University of Mashhad*, p.7.

Moran, M. S., Peters-Lidard, C. D., Watts, J. M., & McElroy, S. (2004). Estimating soil moisture at the watershed scale with satellite-based radar and land surface models. *Canadian journal of remote sensing*, *30*(5), 805-826.

Myrmzlomi, S.M., & Sahebi, Mrs. (2014). Estimation of soil moisture content using SAR data with emphasis on surface re-diffusion models. *PhD thesis of Civil Engineering, Mapping Engineering, Khaje Nasir-e-Din Tusi University of Technology*, P.110.

Nourouzi, A. E., Behbahani, S., Rahimi, K. A., & Aghighi, H. (2008). Surface Soil Moisture Model with NDVI (Case Study: Rangelands of Khorasan Province), *Journal of Environmental Studies*, *48*, 127-136.

P., Matgen, J., Martínez-Fernández, P., Llorens, J., Latron, C., & Martin, M., (2011). Soil moisture estimation through ASCAT and AMSR-E sensors: An intercomparison and validation study across Europe. *Remote Sensing of Environment*, *115*(12), 3390–3408.

Potin, P. (2011). Sentinel-1 Mission Overview Advanced Course on Radar Polarimery, *ESRIN, Frascati*.

Sanli, F.B., Kurucu, Y., Esetlili, M. T, & Abdikana, S. (2008). Soil moisture estimation from RADARSAT-1, ASAR and PALSAR data in agricultural fiels of Menemen plain of western Turkey. *The International Archives of the Photogrammetry, Remote Sensing and Spatial Information Sciences*. Part B7, Beijing.

Silva, A. T., Portela, M. M., Naghettini, M., & Fernandes, W. (2017). A Bayesian peaks-over-threshold analysis of floods in the Itajaí-açu River under stationarity and nonstationarity. *Stochastic environmental research and risk assessment*, *31*(1), 185-204.

Thain, C., Barstow, R., Ramsbottom, D., Lim, P., & Wong, T. (2011). Sentinel-1Product Specification, Ref: S1-RS-MDA-52-744, *Issue/Revision*: 2/2.